

01,05,03,04

## The half-metallic properties of Heusler alloys $Mn_2ScZ$ ( $Z = Al, Si, P, Ga, Ge, As, In, Sn, Sb$ ): ab initio study

© D.R. Baigutlin<sup>1</sup>, V.V. Sokolovskiy<sup>1,2</sup>, O.N. Miroshkina<sup>1,3</sup>, V.D. Buchelnikov<sup>1,2</sup>

<sup>1</sup> Chelyabinsk State University,  
Chelyabinsk, Russia

<sup>2</sup> National University of Science and Technology „MISIS“,  
Moscow, Russia

<sup>3</sup> Duisburg-Essen,  
Duisburg, Germany

E-mail: d0nik1996@mail.ru

Received July 8, 2021

Revised July 8, 2021

Accepted July 8, 2021

The properties of Heusler alloys of the  $Mn_2ScZ$  family ( $Z = Al, Si, P, Ga, Ge, As, In, Sn, Sb$ ) are investigated within the framework of the density functional theory. The PBE GGA and meta-GGA SCAN functionals were used for approximation of the exchange-correlation interactions. Calculations show that PBE does not predict ideal half-metallic behavior, unlike SCAN. It is shown that at  $Z = P, Si$ , a transition from the half-metallic state to the metallic one is observed. This effect can be used to develop tunable spintronic devices.

**Keywords:** exchange-correlation functional, meta-GGA SCAN, half-metal ferromagnets, Heusler alloys.

DOI: 10.21883/PSS.2022.13.52300.18s

### 1. Introduction

Modern tasks require high performance and fast execution of programs, meanwhile electronics is about to reach its physical limit. Therefore, use of other physical effects for storage and transmission of information is interesting. In particular, there is active growth of studies in the area of spintronics. Spintronics is based on the possibility of manipulating spin degrees of freedom of the charge carriers, resulting in flow of spin-polarized current and, as a consequence, spin-dependent physical effects (such as, e.g. magnetoresistive effect and spin carry-over effect) [1,2].

Criteria of efficiency of a spintronic device are the degree of spin polarization of current and the length of spin diffusion of the charge carriers. Spin polarization of current can be reached by means of various physical effects, such as injection of spin from ferromagnetic, application of magnetic or electric field, Zeeman splitting, thermal gradient and mechanical rotation [3]. One of the most common methods is spin injection from ferromagnetic material, e.g. usual ferromagnetic metals (Fe, Co, Ni and Gd) or half-metallic ferromagnetics. The publications provide information on prediction of the half-metallic behavior for various types of materials, such as magnetic oxides [4], diluted semiconductors based on magnetic compounds of the groups III–V of periodic system of chemical elements [5] and Heusler alloys [6]. Among half-metallic ferromagnetics semi- and full Heusler alloys are of big interest, because they usually demonstrate stable half-metallicity, high Curie temperature and a high spin polarization [6].

The potential of Heusler compounds as half-metallic ferromagnetic materials has been known for more than 20 years, since when two groups of scientists Coubler et al demonstrated that for  $Co_2MnAl$  and  $Co_2MnSn$  alloys the spin-downward density of states at the Fermi level of energy is almost zero [7]. At the same time Grut et al obtained similar results for Heusler semi-alloys  $NiMnSb$ ,  $PtMnSb$ ,  $PdMnSb$  and  $PtMnSn$  [8].

Today, the most experimentally and theoretically studied ferromagnetic alloys are  $Co_2YZ$  ( $Y = Fe, Mn$  and  $Z = Si, Ge, Sn, Al$ ) [9–11],  $Fe_2YZ$  ( $Y = Cr, Mn, Co, Ti$  and  $Z = Si, Al, Ga$ ) [12–14] and ferrimagnetic alloys  $Mn_2YZ$  ( $Y = V, Cr, Fe, Co, Ni$  and  $Z = Al, Ga, Si, Ge, Sn, In$ ) [15,16]. It should be noted that Co, Fe and Mn are 3d-metals, therefore, the alloys based on them are highly correlated. Thus, when studying the properties of Heusler alloys it is very important to correctly select the exchange-correlation functionality. The work [17] studied the alloy  $Co_2FeAl$  by using the functionalities GGA and GGA +  $U$  for  $L2_1$  and  $X_A$  crystalline lattices. In  $L1_2$ -phase the alloy demonstrates half-metallic behavior with integer magnetic moment satisfying the Slater–Pauling rule, both for GGA, and with the Hubbard correction GGA +  $U$ , however, the width of the prohibited zone is increased when taking strong correlations into account. For  $X_A$ -structure when using the functionality GGA the alloy  $Co_2FeAl$  demonstrates metallic behavior, nevertheless, the values of spin polarization are quite high. Taking strong correlations into account predicts half-metallic behavior.

Similar data for other family of the Heusler alloys  $Mn_2CoZ$  ( $Z = Al, Ga, Si, Ge, Sb$ ) were obtained by using

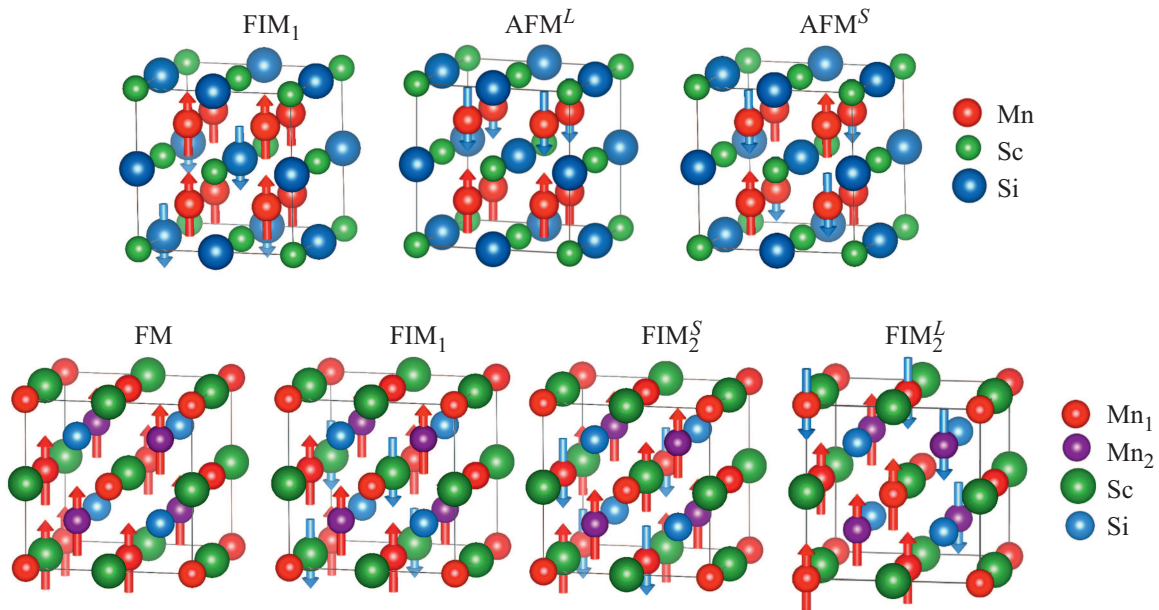


**Figure 1.** Magnet order for L<sub>12</sub>-lattice (top panel) and for X<sub>A</sub>-lattice (bottom panel).

the functionality LDA [18]. Authors have found relation between the stability of structures X<sub>A</sub> and L<sub>21</sub> and the element  $Z$  of main group. In case of  $Z = \text{Al, Ga}$  the structure X<sub>A</sub> is more stable, whereas with  $Z = \text{Si, Ge, Sb}$  direct L<sub>12</sub>-structure turns out more beneficial. It is interesting that half-metallic nature of the alloys Mn<sub>2</sub>CoSi, Mn<sub>2</sub>CoGe and Mn<sub>2</sub>CoSb is stable and senseless to change of the structure type L<sub>12</sub> to X<sub>A</sub>. However, for Mn<sub>2</sub>CoAl and Mn<sub>2</sub>CoGa half-metallic nature disappears during transition from X<sub>A</sub>- to L<sub>12</sub>-structure.

In addition to the type of crystalline structure, external pressure also impacts to half-metallic properties of alloy. For example, for alloy Fe<sub>2</sub>TiSb with increase of the lattice parameter from 5.6 to 6.1 Å ( $\approx 8.2\%$ ) spin polarization is decreased only by 2% [19]. The same, for Mn<sub>2</sub>RuSi it is shown that ideal half-metallic behavior of the system in equilibrium state disappears in case of pressure increase, and the spin polarization coefficient ( $P$ ) is 37% at 100 GPa [20]. Inversely, impact of pressure may stabilize half-metallic structure. Thus, alloy Co<sub>2</sub>TiGa transits from metallic state to half-metallic at the pressure 10 GPa (1.6% lattice compression), further pressure increase up to 25 GPa makes the alloy [21] metallic again.

Of all half-metallic alloys Mn<sub>2</sub>YZ it seems to be interesting to consider the alloys Mn<sub>2</sub>ScZ, because Sc has only one valent  $3d$ -electron, and, therefore, it is the simplest one in terms of the electron structure. Moreover, alloys Mn<sub>2</sub>ScZ ( $Z = \text{Si, Ge, Sn}$ ) were recently studied by Ram et al within the framework of the density functional theory subject to strong correlations in the Hubbard model [22]. In this regard, the purpose of this work is prediction of new half-metallic ferromagnetic materials based on Heusler alloys of the Mn<sub>2</sub>ScZ family ( $Z = \text{Al, Si, P, Ga, Ge, As, In, Sn, Sb}$ ) of stoichiometric composition for application in the

spintronic devices subject to strong correlations taken into account by using non-parametrical half-local functionality SCAN belonging to the group meta-GGA [23].

## 2. Analysis details

Geometrical optimization of the lattice was performed within the framework of the density functional theory by using the projector augmented waves approach implemented in the VASP software package [24,25]. Exchange-correlation effects are taken into account by using the functionalities GGA-PBE [26] and meta-GGA SCAN [23].  $k$ -the grid was generated automatically according to the Monkhorst-Pack scheme and was  $11 \times 11 \times 11$   $k$ -points for relaxation, and  $25 \times 25 \times 25$   $k$ -points for accurate calculations of the density of electron states (DOS). The flat waves cutting energy was 800 eV, and the energy convergence parameter was  $10^{-8}$  eV/atom.

Spin polarization was calculated by using the formula

$$P = \frac{|N_{\uparrow} - N_{\downarrow}|}{N_{\uparrow} + N_{\downarrow}}, \quad (1)$$

where  $N_{\uparrow}, N_{\downarrow}$  — density of electron states with the spin upward and downward, accordingly.

## 3. Results and discussion

At the first stage we performed geometric optimization of the lattice for L<sub>12</sub>- and X<sub>A</sub>-structures having ferromagnetic (FM), ferrimagnetic (FIM) or antiferromagnetic (AFM) order, as shown in Fig. 1.

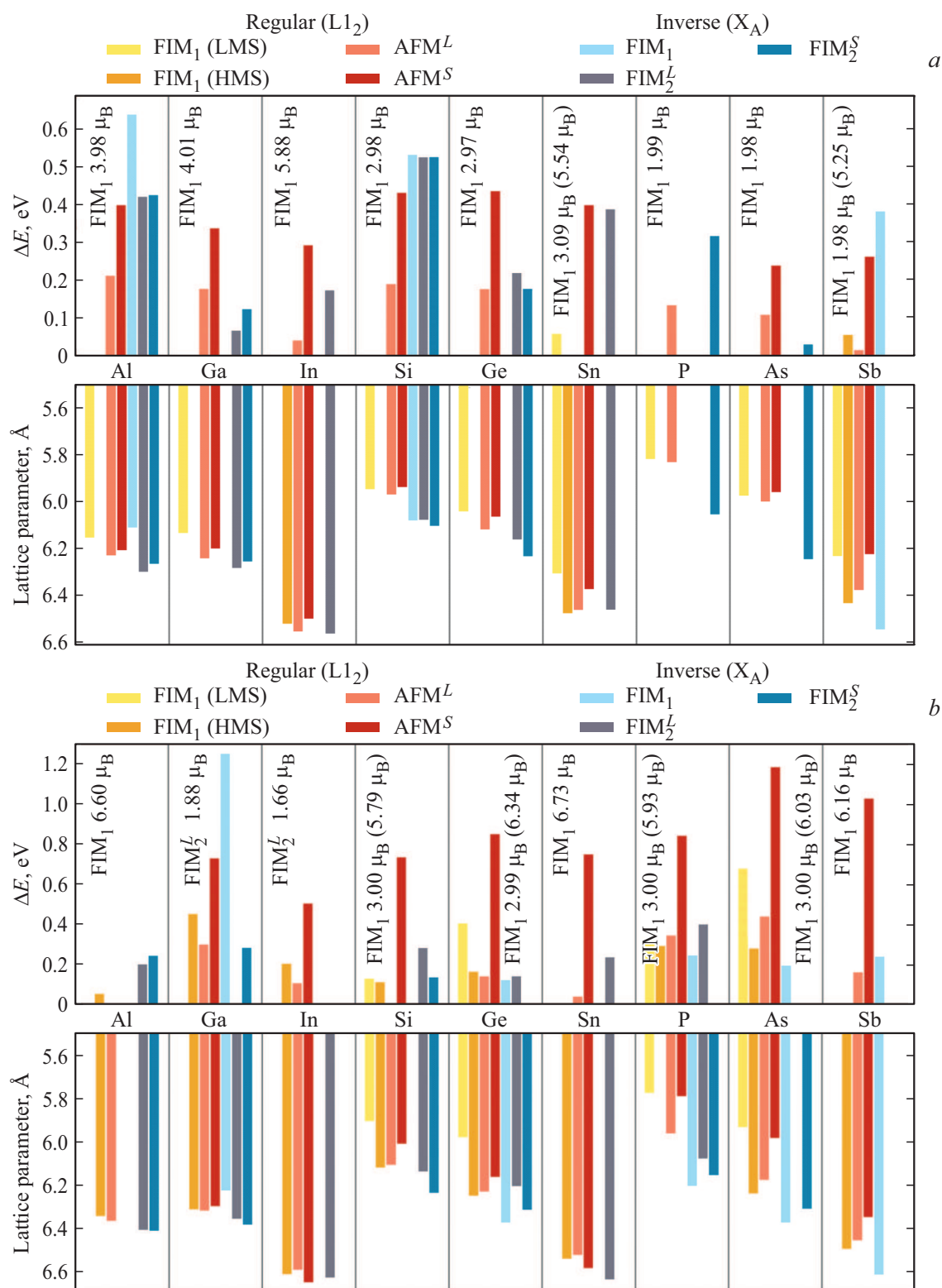


**Figure 2.** Dependence of the difference of energies  $\Delta E$  of various magnetic phases on the equilibrium phase energy (specified in Figure with the values of total magnetic moment) and parameter of the phase lattice (a) for the functionality PBE and (b) for the functionality SCAN in alloys  $\text{Mn}_2\text{ScZ}$  on the element Z ( $Z = \text{Al, Si, P, Ga, Ge, As, In, Sn, Sb}$ ) for the lattices  $L1_2$  and  $X_A$ . For the alloys, in which two energy minimums are implemented, there are two values of magnetic moments.

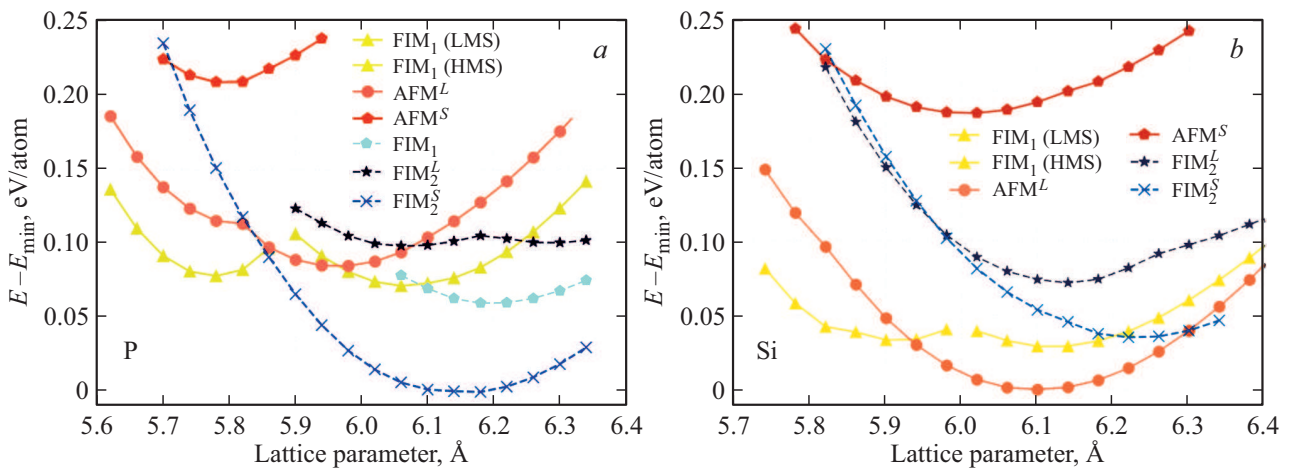


**Figure 3.** Dependence of the difference of energies of various magnetic phases on the lattice parameter for  $Mn_2ScP$  and  $Mn_2ScSi$  calculated by using the functionality SCAN. Solid line corresponds to  $L_{12}$ -lattice, dotted line —  $X_A$ -lattice.

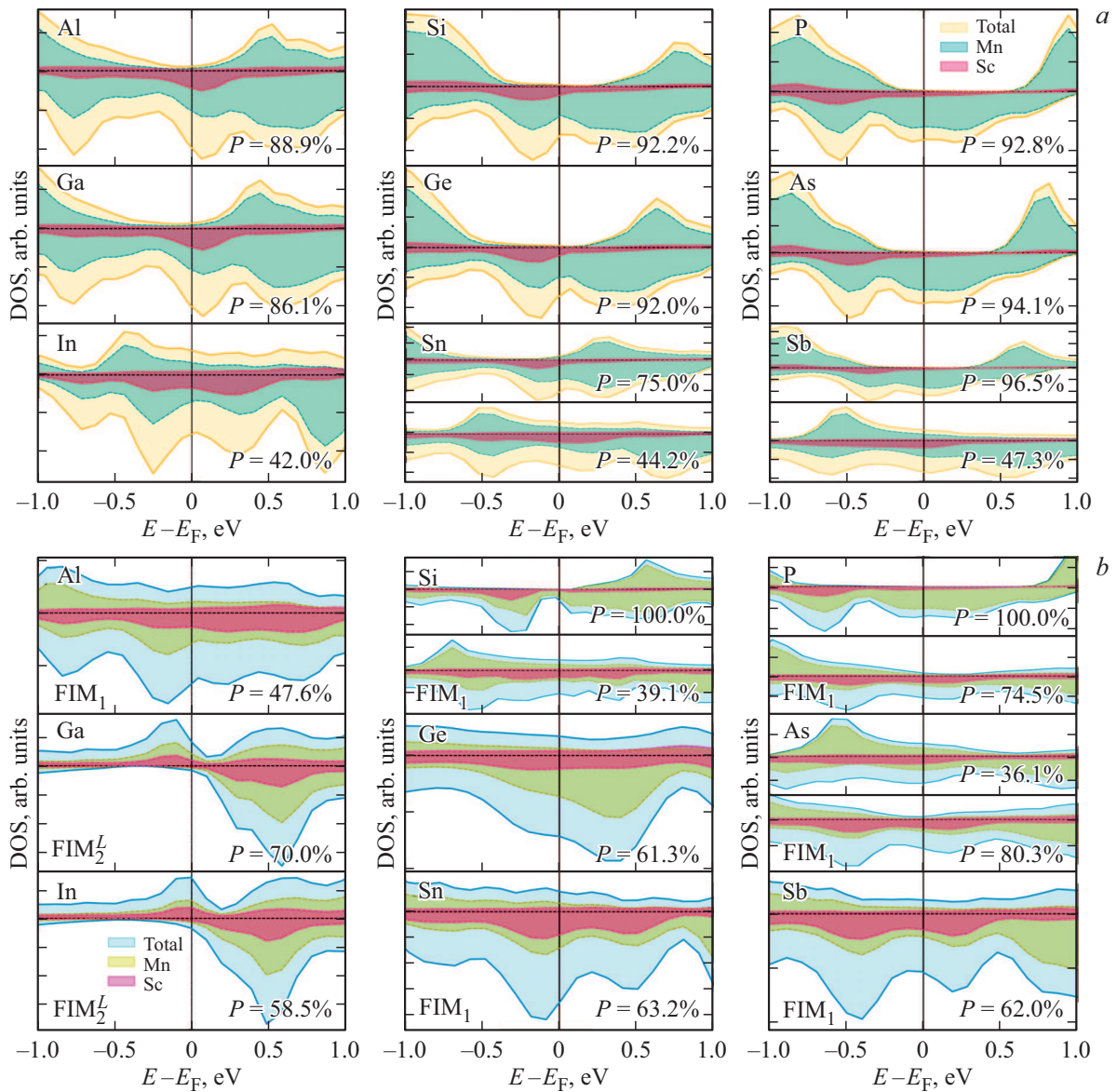


**Figure 4.** The density of electron states  $Mn_2ScZ$  ( $Z = Al, Si, P, Ga, Ge, As, In, Sn, Sb$ ) calculated by using the functionalities PBE (a) and SCAN (b) for the energy-beneficial ferrimagnetic order. Digits refer to the degree of polarization  $P$ .

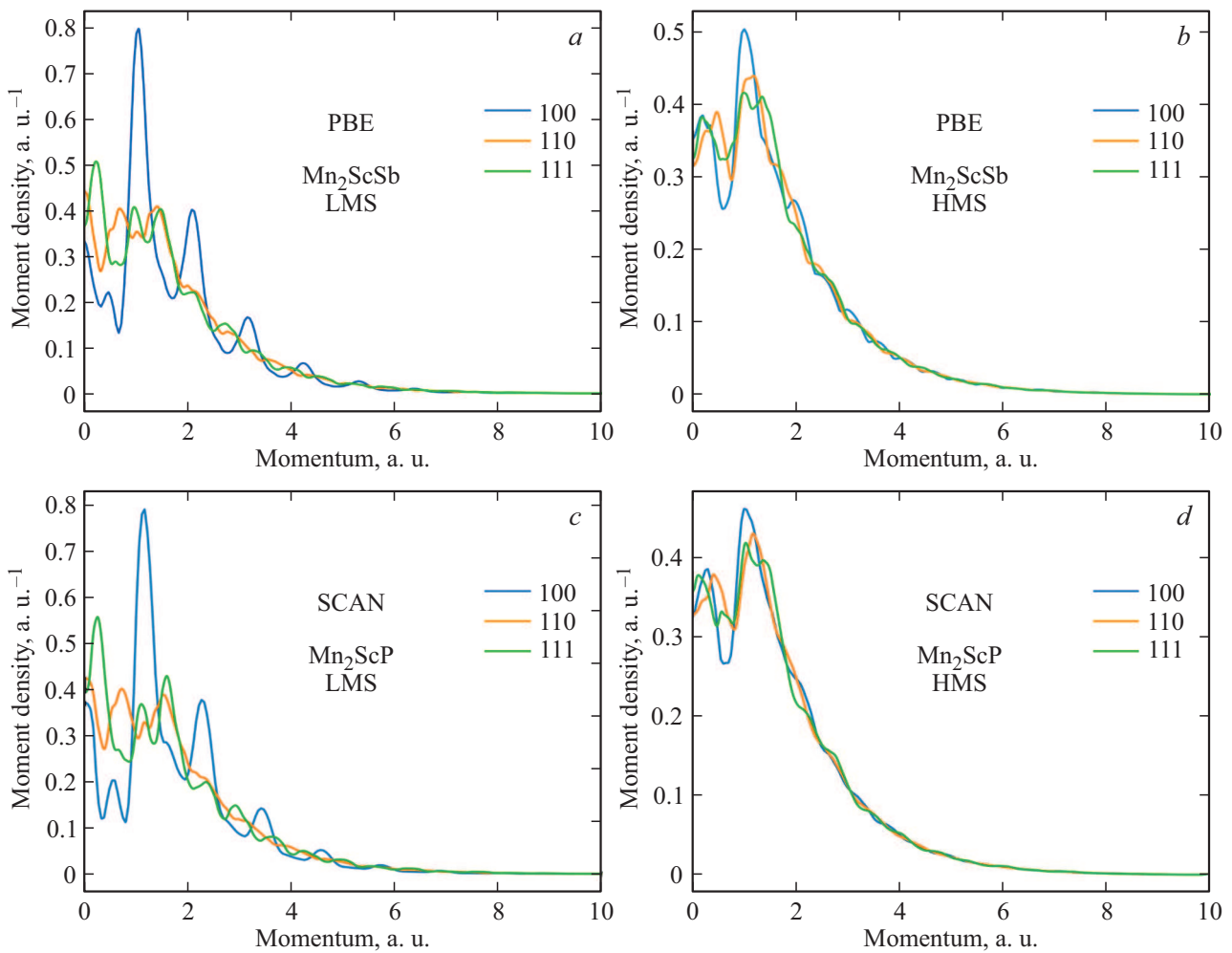


**Figure 5.** Profiles of Compton magnetic scattering for various crystallographic directions in  $\text{Mn}_2\text{ScSb}$  for LMS- and HMS-states PBE (*a, b*) and  $\text{Mn}_2\text{ScP}$  for LMS- and HMS-states SCAN (*c, d*).

Fig. 2 shows dependence of the energy normalized to the minimum energy for that composition, on the lattice parameter. Analyses show that in case of PBE functionality in alloys  $\text{Mn}_2\text{ScSn}$  and  $\text{Mn}_2\text{ScSb}$  dependence of the energy on the lattice parameter has two minimums with different values of the magnetic moment — low moment state (LMS) and high moment state (HMS). In this case Fig. 2 for equilibrium magnetic configuration shows the difference of energies between LMS and HMS. Similar behavior is demonstrated by alloys  $\text{Mn}_2\text{ScSi}$ ,  $\text{Mn}_2\text{ScGe}$ ,  $\text{Mn}_2\text{ScP}$  and  $\text{Mn}_2\text{ScAs}$  when using the functionality SCAN.

In case of the functionality PBE beneficial one is  $L1_2$ -lattice with  $\text{FIM}_1$  magnetic order. Total magnetic moment in LMS is virtually whole; it satisfies the Slater–Pauling rule, which is necessary, but not sufficient condition of presence of half-metallic state in the compound.

For the functionality SCAN equilibrium magnetic structure strongly depends on Z-element. For the most of alloys, except for  $Z = \text{Al}, \text{Si}, \text{Sn}, \text{Sb}$ , reverse lattice  $X_A$  is beneficial. At  $Z = \text{Si}, \text{Ge}, \text{P}, \text{As}$  two (LMS and HMS) energy minimums are realized. SCAN predicts the whole

magnetic moment for LMS. It is also interesting that in case of  $Z = \text{Si}, \text{P}$  energetic barrier between LMS and HMS is quite small, which indicates the possibility of transition between these two states (Fig. 3).

For both used functionalities equilibrium lattice parameter is increased in case of transition to the next line of Mendeleev’s table, and remains virtually constant within the framework of one period, which most likely associated with increase of atomic radius of Z-element.

To study the electron structure and half-metallic characteristics of alloy we calculated total and element-by-element densities of electron states (DOS and pDOS) for the most beneficial ferrimagnetic structure. These are shown in Fig. 4.

In Fig. 4, *a* you can see that the degree of spin polarization is quite high, in those cases when the alloy is in LMS  $\text{FIM}_1$  with almost whole magnetic moment. However, for the functionality PBE, spin polarization at Fermi level does not reach 100%. Therefore, without strong correlations it is impossible to predict ideal half-metallic state of Heusler alloys observed experimentally [27,28].

The most interesting are alloys  $Mn_2ScSi$  and  $Mn_2ScP$ , because there are two virtually degraded states observed for them with 100% and low spin polarization, accordingly. Such materials feature metallic behavior with regard to spin-downward electrons, meanwhile for the spin-upward electrons there is an energy slot, in case when the alloy has  $FIM_1$  LMS-order. Therefore,  $Mn_2ScZ$  ( $Z = Si, P$ ) in half-metallic state are ferromagnetic semimetals of  $I_B$  [6] type, as the majority of Heusler alloys [5,6]. On the other hand, with increase of the parameter of lattice the alloy turns to HMS-phase featuring metallic state. Also it is interesting, that for  $Z = Ga, In$  beneficial state is  $X_A$ -lattice with  $FIM_2$ -order, which has a pseudoslot, but it is in the spin-downward channel.

As you can see in Fig. 4 pDOS Sc virtually does not make contribution into the density of states near to the Fermi level, especially for spin-upward channel, therefore, Mn plays a definitive role in appearance of half-metallic properties in that class of alloys. The energy slot appears as a result of hybridization of  $d$ -states between neighboring Mn atoms. Hybrid Mn — Mn-orbitals may not connect to  $d$ -orbitals of Sc due to their different symmetry, and a gap is generated between these not connecting orbitals, which can be seen by DOS peaks at the edge of valence band and the conductivity band. Similar reasons for generation of semiconductor slot in whole Heusler alloys were observed in  $Co_2MnGe$ ,  $Mn_2ScZ$  and ( $Z = Si, Ge, Sn$ ) [22,29].

The value of magnetic moment and the degree of polarization can be determined based on the profiles of Compton magnetic scattering. Fig. 5 shows profiles of Compton magnetic scattering in various directions calculated by using the functionality PBE for  $Z = Sb$  and the functionality SCAN for  $Z = Si$ . It is seen that for LMS there is heavy anisotropy, which becomes far lower during transition to HMS-phase. For LMS-phase there is a central fall, which can be caused by negatively polarized electrons of conductivity [30,31].

## 4. Conclusion

By using methods of the density functional theory we studied properties of the alloys  $Mn_2ScZ$  ( $Z = Al, Si, P, Ga, Ge, As, In, Sn, Sb$ ). With strong correlations taken into account by using the functionality SCAN for the alloys  $Mn_2ScSi$  and  $Mn_2ScP$  we predicted semi-metal to metal switchable behavior in case of increase of the lattice parameter. This mechanism can be useful for development of spintronic devices, such as spin filters, sensors, switches, and logic valves.

## Work funding

The study was carried out with the financial support of the Russian Foundation for Basic Research and the Chelyabinsk Region under the scientific project No. 20-42-740006.

## Conflict of interest

The authors declare that they have no conflict of interest.

This article does not contain any researches with participation of a human as the object of studies.

## References

- [1] G. Binasch, P. Grunberg, F. Saurenbach, W. Zinn. *Phys. Rev. B* **39**, 4828 (1989).
- [2] J.M. Kikkawa, I.P. Smorchkova, N. Samarth, D.D. Awschalom. *Science* **277**, 1284 (1997).
- [3] A. Hirohata, K. Takashi. *J. Phys. D* **47**, 193001 (2014).
- [4] S.P. Lewis, P.B. Allen, T. Sasaki. *Phys. Rev. B* **55**, 16, 10253 (1997).
- [5] H. Akai. *Phys. Rev. Lett.* **81**, 14, 3002 (1998).
- [6] C. Felser, G.H. Fecher, B. Balke. *Angew. Chem. Int. Ed.* **46**, 5, 668 (2007).
- [7] J. Kubler, A.R. Williams, C.B. Sommers. *Phys. Rev. B* **28**, 1745 (1983).
- [8] R.A. de Groot, F.M. Mueller, P.G. van Engen, K.H.J. Buschow. *Phys. Rev. Lett.* **50**, 2024 (1983).
- [9] D. Hoat, J. Rivas-Silva, A.M. Blas. *J. Comput. Electron.* **17**, 1470 (2018).
- [10] B. Deka, D. Chakraborty, A. Srinivasan. *Physica B* **448**, 173 (2014).
- [11] L. Siakeng, G.M. Mikhailov, D. Rai. *J. Mater. Chem. C* **6**, 10341 (2018).
- [12] S. Chaudhuri, V. Srihari, A. Nigam, P. Bhoje. *J. Appl. Phys.* **126**, 083904 (2019).
- [13] S. He, Y. Liu, Y. Zheng, Q. Qin, Z. Wen, Q. Wu, Y. Yang, Y. Wang, Y. Feng, K.L. Teo, C. Panagopoulos. *Phys. Rev. Mater.* **1**, 064401 (2017).
- [14] L. Hongzhi, Z. Zhiyong, M. Li, X. Shifeng, L. Heyan, Q. Jingping, L. Yangxian, W. Guangheng. *J. Phys. D* **40**, 7121 (2007).
- [15] H. Luo, Z. Zhu, G. Liu, S. Xu, G. Wu, H. Liu, J. Qu, Y. Li, J. Magn. Magn. Mater. **320**, 421 (2008).
- [16] V.V. Sokolovskiy, M.A. Zagrebin, Y. Sokolovskaya, V.D. Buchelnikov. *Solid State Phenom.* **233**, 229 (2015).
- [17] R. Jain, N. Lakshmi, V.K. Jain, V. Jain, A.R. Chandra, K. Venugopalan. *J. Magn. Magn. Mater.* **448**, 278 (2018).
- [18] G.D. Liu, X.F. Dai, H.Y. Liu, J.L. Chen, Y.X. Li, G. Xiao, G.H. Wu. *Phys. Rev. B* **77**, 014424 (2008).
- [19] H. Luo, G. Liu, F. Meng, J. Li, E. Liu, G. Wu. *J. Magn. Magn. Mater.* **324**, 20, 3295 (2012).
- [20] T. Song, Q. Ma, X.W. Sun, Z.J. Liu, X.P. Wei, J.H. Tian. *J. Magn. Magn. Mater.* **424**, 359 (2017).
- [21] A. Amudhavalli, R. Rajeswarapalanichamy, K. Iyakutti. *Phase Transitions* **92**, 9, 875 (2019).
- [22] M. Ram, A. Saxena, A.E. Aly, A. Shankar. *RSC Advances* **10**, 13, 7661 (2020).
- [23] J. Sun, A. Ruzsinszky, J.P. Perdew. *Phys. Rev. Lett.* **115**, 3, 036402 (2015).
- [24] G. Kresse, J. Furthmüller. *Phys. Rev. B* **54**, 11169 (1996).
- [25] G. Kresse, D. Joubert. *Phys. Rev. B* **59**, 1758 (1999).

- [26] J. Perdew, K. Burke, M. Ernzerhof. Phys. Rev. Lett. **77**, 3865 (1996).
- [27] H. Itoh, T. Nakamichi, Y. Yamaguchi, N. Kazama. Trans. Jpn. Inst. Met. **24**, 265 (1983).
- [28] C. Jiang, M. Venkatesan, J.M.D. Coey. Solid State Commun. **118**, 513 (2001).
- [29] I. Galanakis, P.H. Dederichs, N. Papanikolaou. Phys. Rev. B: Condens. Matter Mater. Phys. **66**, 17, 174429 (2002)
- [30] A. Dashora, B.L. Ahuja, A. Vinesh, N. Lakshmi, M. Itou, Y. Sakurai. J. Appl. Phys. **110**, 1, 013920 (2011).
- [31] A. Deb, M. Itou, Y. Sakurai, N. Hiraoka, N. Sakai. Phys. Rev. B. **63**, 6, 064409 (2001).